Epilepsy Research 152 (2019) 42–51

Contents lists available at ScienceDirect

Epilepsy Research

journal homepage: www.elsevier.com/locate/epilepsyres

Effective connectivity analysis of iEEG and accurate localization of the epileptogenic focus at the onset of operculo-insular seizures

Elie Bou Assi[a,*], Sandy Rihana[b], Dang K. Nguyen[c,1], Mohamad Sawan[a,1]

[a] Polystim Neurotech Lab, Institute of Biomedical Engineering, Polytechnique Montreal, Montreal, QC, Canada
[b] Biomedical Engineering Department, Holy Spirit University of Kaslik (USEK), Jounieh, Lebanon
[c] University of MontrealHospital Center (CHUM), University of Montreal, Montreal, QC, Canada

ARTICLE INFO

Keywords:
Insular epilepsy
Effective connectivity
Intracranial electroencephalography
Autoregressive modeling
Spectrum weighted adaptive directed transfer function

ABSTRACT

Recognition of insular epilepsy may sometimes be challenging due to the rapid speed at which insular seizures can spread throughout the cortex via extensive connections to surrounding cortices. The spectrum weighted adaptive directed transfer function, a multivariate causality-based effective connectivity measure, was applied to intracranial electroencephalography recordings to identify generators of seizure activity. A non-parametric test based on surrogate data testing was used to validate statistical significance of causal relations. Outflow and inflow of seizure activity were extracted from the computed transfer matrix. Recorded data of 21 seizures from seven patients were analyzed including five who were rendered seizure-free after operculo-insular resection. Effective connectivity analysis of 7 s following electrical onset confirmed an operculo-insular seizure origin in 5 patients with a good post-operative seizure outcome, and for whom the resected region was sampled by intracranial electroencephalography contacts. Different or additional seizure foci were identified in 2 patients with a bad post-operative seizure outcome. Findings highlight the feasibility of accurate operculo-insular seizure foci localization based on quantitative approaches.

1. Introduction

Epilepsy is a chronic condition characterized by recurrent seizures (or 'ictus') resulting from abnormal and excessive neuronal discharges. When antiepileptic drugs fail to control seizures, surgical resection of the epileptic focus is recommended if it can be delineated by a set of tests which often include qualitative visual interpretation of intracranial electroencephalography (iEEG) recordings of seizures. Several authors have recently applied quantitative effective connectivity analyses on such recordings to characterize the complex epileptic network of the different brain areas involved in the generation, propagation, and modulation of seizures. By exploiting temporal precedence among a set of signals to reveal information transfers from 'driver' to 'secondary' nodes of the network, effective connectivity analyses may help understand seizure semiology and optimize delineation of the area to be resected for seizure cure (Jia et al., 2014; van Mierlo et al., 2013). Until now, such methods have mainly been used to analyze temporal or frontal lobe seizures (Klamer et al., 2015; Martinez-Vargas et al., 2017; van Mierlo et al., 2013; Wilke et al., 2010). While little attention has been given to insular seizures (Hagiwara et al., 2017), effective connectivity measures could possibly help explain the diversity in their ictal symptoms and facilitate their identification knowing how complex their ictal intracranial EEG patterns can be (often with the involvement of several distinct structures in as much that visual identification of the area of seizure onset is difficult) (Levy et al., 2017).

Highly connected to surrounding frontal, temporal and parietal lobes (Ghaziri et al., 2017), the insula is a multimodal area involved in the processing of several sensory stimuli (viscerosensory, somatosensory, auditory, gustatory, and olfactory) and cognitive processes (attention, social cognition, and decision-making) (Uddin et al., 2017). Such structural and functional connectivity considerations may explain why insular seizures are diverse in terms of EEG patterns but also in clinical presentation such as early viscerosensory auras (common in temporal lobe seizures), somatosensory auras (as in parietal lobe seizures) and hypermotor symptoms (resembling frontal lobe seizures) (Obaid et al., 2017). Such mimicry has most likely misled some clinicians into thinking that their patients, suffering from insular epilepsy,

* Corresponding author at: Polystim Neurotech Lab (polystim.org), Institute of Biomedical Engineering, Polytechnique Montreal (polymtl.ca), 2900, boul. Édouard-Montpetit, Université de Montréal Campus, 2500, Chemin de Polytechnique, Room M5306, Lassonde Building, Montréal, QC, H3T 1J4, Canada.
E-mail address: elie.bou-assi@polymtl.ca (E. Bou Assi).
[1] Equally contributing PIs.

https://doi.org/10.1016/j.eplepsyres.2019.02.006
Received 28 July 2018; Received in revised form 23 December 2018; Accepted 21 February 2019
Available online 11 March 2019
0920-1211/

had temporal, frontal or parietal lobe seizures leading to the resection of the wrong cortical area (Harroud et al., 2012).

A long list of measures has been proposed for the study of effective connectivity and neuronal network dynamics. Compared to bivariate measures, multivariate approaches showed more accurate performances in estimating causal relations during seizure initiation and spread (Assi et al., 2016; Kaminski et al., 2001). Directed transfer function (DTF), a multivariate directional connectivity measure, has been validated for quantifying causal relations when quasi-stationarity requirements of EEG signals are met (He et al., 2011; Wilke et al., 2010). Although quasi-stationary EEG signals can be identified when analyzing a relatively small number of electrodes, it is more difficult when dealing with a higher number of electrodes. To cope with stationarity issues, Wilke et al. (2008) proposed the Adaptive Directed Transfer Function (ADTF), a time varying version of the DTF (Wilke et al., 2008).

However, for both DTF and ADTF, visual analysis remained necessary for identifying frequency ranges of interest. Subsequently, the spectrum weighted ADTF (swADTF) was proposed, taking into account the full frequency range of the signal and weighting each element of the transfer matrix by the sending channel's auto spectrum (Martinez-Vargas et al., 2017; van Mierlo et al., 2013). In this study, we investigate the effective connectivity of apparent operculo-insular seizures of different semiology using the swADTF.

2. Materials and methods

Fig. 1 shows the block diagram of the implemented swADTF-based connectivity analysis framework. High-density iEEG recordings following onset of ictal seizure activity were first selected. Connectivity between iEEG electrodes was obtained by applying the swADTF to iEEG time series. Statistical validation was performed by means of surrogate data testing. Outflow and inflow values were quantified, and seizure activity sources and sinks were identified.

2.1. Patients

Intracranial EEG recordings of seven patients diagnosed with insulo-opercular epilepsy were retrospectively analyzed (Table 1). Patients were selected based on the following inclusion criteria: (1) seizure onset zone located within the insula (with or without extension to the adjacent operculum) as assessed by the clinician of the iEEG study; (2) iEEG electrodes sampled the insula, opercula, as well as temporal, parietal or frontal structures. In 5 patients, focal cortical resection of the seizure onset zone resulted in a good seizure outcome (Engel I) with at least two years of follow-up. The two remaining patients had a poor outcome (Engel IIIA). The Engel epilepsy surgery outcome scale was used to classify postoperative outcomes (Engel, 1993).

Raw iEEG signals were acquired using the Harmonie monitoring system (Stellate Systems Inc.), sampled at 2000 Hz and filtered at

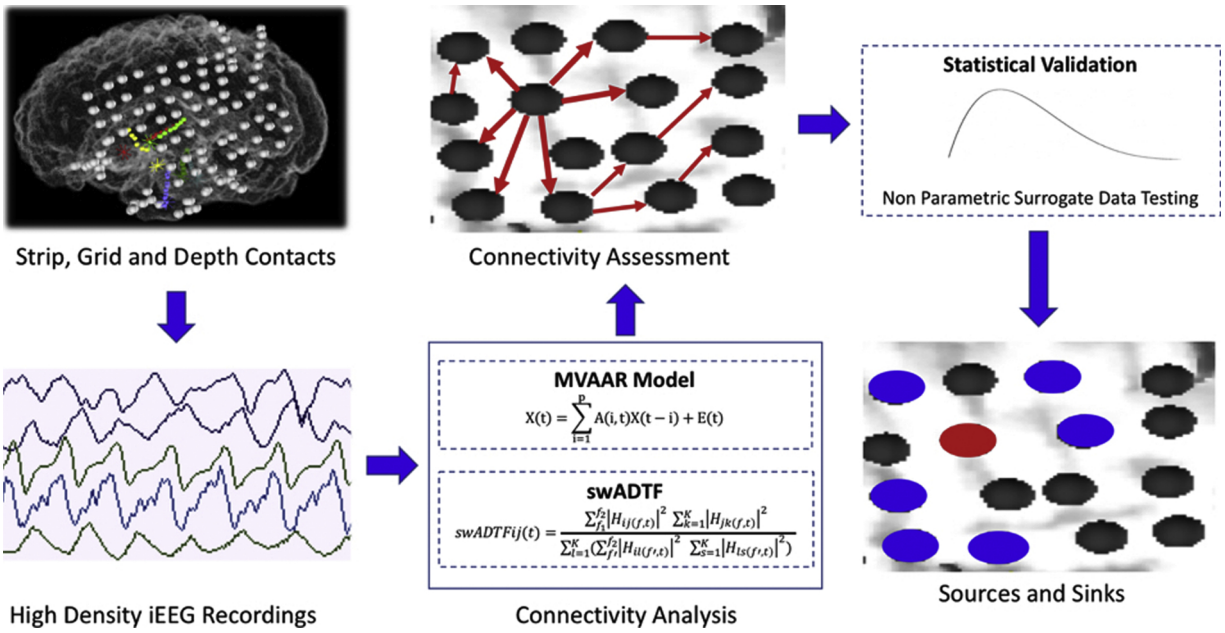

Fig. 1. Framework of the swADTF-based connectivity implementation (iEEG: intracranial electroencephalography; MVAAR: multivariate adaptive autoregressive model; swADTF: spectrum weighted adaptive directed transfer function).

Table 1
Clinical characteristics of patients.

Patient ID	Gender	Age	Epilepsy duration (Y)	SOZ	Side	MRI	# of iEEG contacts	Outcome (Engel)	Follow-up (years)
1	F	38	33	aINS + F op	L	N	110	IA	5
2	M	36	7	pIINS	L	N	61	IB	4
3	M	35	10	supINS + F op	R	N	100	IA	7
4	M	46	31	pINS, P op/T op	L	N	91	IA	5
5	F	18	9	sup INS, F op	L	N	114	IA	2
6	F	32	11	pINS, T op/P op	R	N	74	IIIA	5
7	M	36	5	aINS, F op	R	N	112	IIIA	2

F: female; M: male; Y: years; SOZ: seizure onset zone; aINS: anterior insula; F op: frontal operculum; pINS: posterior insula; supINS: superior insula; P op: parietal operculum; T op: temporal operculum; L: left; R: right, MRI: magnetic resonance imaging, N: normal; Engel IA: completely seizure-free after surgery; Engel IB: only non-disabling simple partial seizures after surgery; Engel IIIA: worthwile seizure reduction.

500 Hz. Table 1 summarizes patients' clinical characteristics. The research protocol was approved by the University of Montreal Hospital Research Center ethical committee.

2.2. Spectrum weighted adaptive directed transfer function

For each patient, three iEEG-recorded seizures were randomly chosen and analyzed using swADTF. Electrical onset (before regional propagation and spread) was marked by an expert epileptologist. All available iEEG channels were included in the effective connectivity analysis. Given the relatively high number of contacts and that iEEG recordings before synchronous ictal activity are not necessarily stationary, an adaptive multivariate autoregressive modeling was preferred. The ADTF allows investigating time-varying connectivity patterns and does not entail stationarity requirements. It is based on a multivariate adaptive auto regressive model (MVAAR) (Wilke et al., 2008) (1):

$$\boldsymbol{X}(t) = \sum_{i=1}^{p} \boldsymbol{A}(i,t)\boldsymbol{X}(t-i) + \boldsymbol{E}(t) \quad (1)$$

where $X(t)$ is a multivariate signal, $A(i,t)$ is a matrix gathering time varying model coefficients, $E(t)$ is the error matrix and p is the model order. Non-linear Kalman filtering, based on a combination of observation and state space equations, was used to estimate model's time varying coefficients (Wilke et al., 2008). The frequency domain transfer matrix $H_{ij}(f,t)$ is obtained by Fourier transforming Eq. (1). $H_{ij}(f,t)$ displays causal relations from the electrode j to electrode i at time instant t and frequency f. Although the clinical validity of the ADTF has been demonstrated (Wilke et al., 2008), Mierlo et al. (2013) found that at some frequency f and time t, the term $H_{ij}(f,t)$ may be high even though power of signal j is relatively low (van Mierlo et al., 2013).

They subsequently proposed the swADTF in which $H_{ij}(f,t)$ is divided by the auto spectrum of the sending channel (2).

$$\boldsymbol{swADTF_{ij}}(t) = \frac{\sum_{f_1}^{f_2} |\boldsymbol{H}_{ij(f,t)}|^2 \sum_{k=1}^{K} |\boldsymbol{H}_{jk(f,t)}|^2}{\sum_{l=1}^{K} (\sum_{f'=f_1}^{f_2} |\boldsymbol{H}_{il(f',t)}|^2 \sum_{s=1}^{K} |\boldsymbol{H}_{ls(f',t)}|^2)} \quad (2)$$

where $f1$ and $f2$ are frequency bounds of interest, and k is the total number of channels (van Mierlo et al., 2013).

Three seizures per patient were randomly chosen and seizure onset was marked by an expert epileptologist (DKN). For each seizure, an ictal segment from 5 s prior to and 7 s after the labelled onset was selected for analysis. Extracted epochs were bandpass [0.5–40 Hz] filtered using a 6th order zero-phase Butterworth filter.

To avoid any DC bias (which makes a signal nonlinear and thus not amendable to linear fit by an autoregressive model), filtered iEEG signals were standardized (mean subtraction, and standard deviation division). Multivariate autoregressive model orders were adaptively determined by finding the minimum on the Bayesian Information Criterion plot for each individually analyzed seizure (Wilke et al., 2010). Minimum and maximum model order limits were respectively fixed to 1 and 10 with unity increments and an update coefficient of 0.001 was used to compute model coefficients (van Mierlo et al., 2013).

2.3. Surrogate data testing

The swADTF exhibits a highly non-linear relation with the time series from which it is derived resulting in a fairly well-established estimators' distribution under the null hypothesis of no causal interaction. Subsequently, a non-parametric statistical test is required to validate the statistical significance of causal relations among iEEG channels. Surrogate data testing was performed by independently and randomly shuffling Fourier transform phases, thus resulting in a new time series (surrogate). Replicating this operation several times creates an empirical distribution of computed swADTF values under the null hypothesis of no interaction. Statistical significance of causal interactions is then assessed through comparison to the generated empirical/random distribution. In line with earlier investigations, shuffling was repeated 1000 times and a significance level of 0.05 was considered (Wilke et al., 2010).

2.4. Outflow and inflow of seizure activity

Since the swADTF displays causal relations from channel j to channel i, outflow of seizure activity (from channel j to all remaining ones) can be quantified by integrating and normalizing across the transfer matrix's columns (3). Similarly, seizure activity inflow can be determined by repeating the same procedure across the rows of the transfer matrix (4).

$$Outflow = \frac{\sum_{i=1}^{K} swADTF_{ij}}{K} \quad (3)$$

$$Inflow = \frac{\sum_{j=1}^{K} swADTF_{ij}}{K} \quad (4)$$

For $i = 1$ to K, and $j = 1$ to K where K is the total number of channels

High outflow or inflow values indicate that a given electrode can be respectively considered as a source or sink of seizure activity. In line with previous investigations, the electrode contact exhibiting the highest outflow across each analyzed seizure was considered the ictal generator (He et al., 2011; van Mierlo et al., 2013; Wilke et al., 2008, 2010). In contrast, to assess the spread of ictal activity, sinks of seizure activity were electrode contacts exhibiting inflow values higher than 80% the maximal inflow value.

2.5. Synthetic iEEG recordings

The implemented swADTF-based seizure generators/sinks identification framework was first tested on a 9-node simulated connectivity pattern (3 × 3 grid). A primary generator of seizure activity, consisting of real ictal data (sampled at 400 Hz), was propagated to the 8 remaining nodes. This connectivity propagation model was provided as part of the eConnectome Matlab toolbox for mapping and imaging of brain functional connectivity (He et al., 2011) and was previously used to validate other connectivity methods such as the DTF (Wilke et al., 2010) and the ADTF (Wilke et al., 2008). The swADTF was evaluated and integrated across frequency range (4–10 Hz) and whole segment duration. Fig. 2 illustrates the simulated propagation pattern. In order

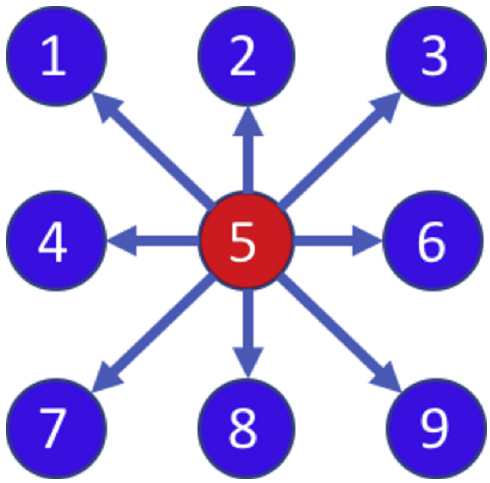

Fig. 2. Graphical node illustration of the simulated propagation pattern. Node 5 was simulated as a generator of seizure activity that propagates to all remaining nodes (sinks).

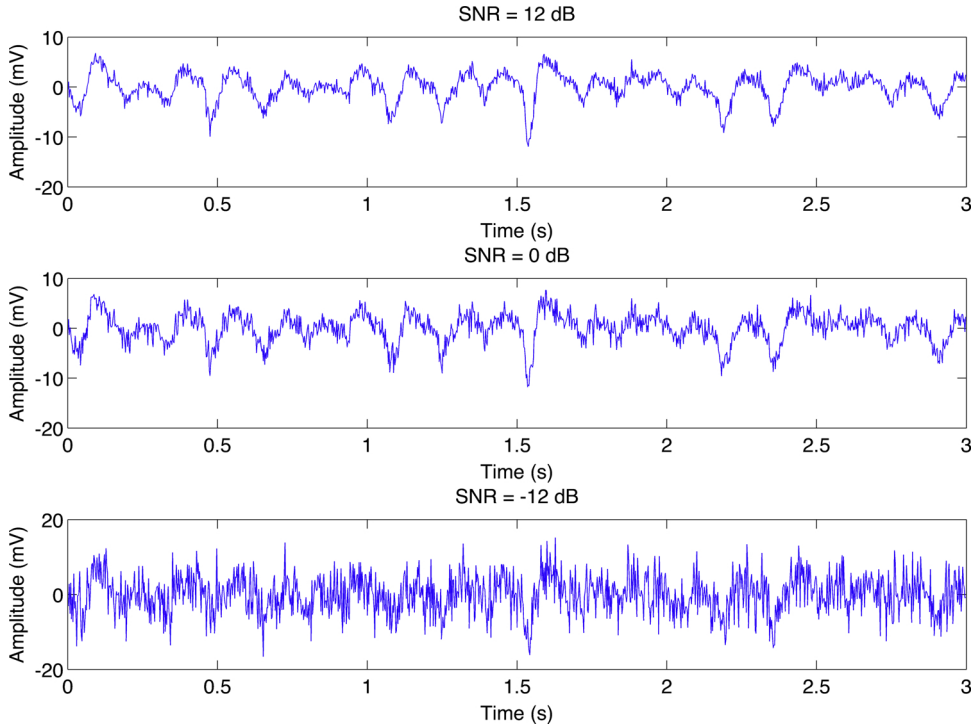

Fig. 3. Illustrative one-channel raw iEEG recordings with different SNRs. top: SNR = 12 dB; middle: SNR = 0 dB; bottom: SNR = −12 dB. A Gaussian white noise was added with SNRs ranging from −12 dB to 12 dB to assess the proposed framework's robustness to noise; SNR: Signal to noise ratio.

to evaluate the resistance of the proposed analytical framework to noise and interference, an additive Gaussian white noise was imposed to iEEG recordings. Recently, Paris et al. (2017) demonstrated that noises interfering with iEEG recordings could be modeled by an additive white Gaussian noise or a causal periodic autoregressive moving average model (Paris et al., 2017).

Different noise levels were added to the generated 9-node connectivity pattern resulting in signal-to-noise ratios (SNR) between −12 dB and 12 dB (unity increments). Fig. 3 displays illustrative raw iEEG recordings with SNRs of 12 dB (top), 0 dB (middle), and −12 dB (bottom).

3. Results

3.1. Simulation results

Fig. 4 displays the transfer function (0 dB noise), in addition to the normalized outflow and inflow of seizure activity as respectively integrated across the columns and lines of swADTF transfer matrix. Electrode 5 can be quantitatively identified as the source of seizure activity confirming the simulated connectivity pattern. In addition, contact 5 exhibited the outflow and lowest inflow values. Remaining electrodes (sinks of seizure activity) displayed low outflow and high inflow values, as expected.

The entire localizing methodology, including surrogate data testing (1000 times shuffling, $\alpha = 0.05$) was applied to the simulated data. As shown in Fig. 5, the swADTF is stable in identifying node 5 as the generator of seizure activity even in the presence of high noise levels.

3.2. Sources of seizure activity - group results

Using the MVAAR model coefficients, swADTF was integrated from $f1 = 3$ Hz to $f2 = 40$ Hz based on Eq. (2). The high cut-off frequency (3 Hz) was chosen in an attempt to exclude low frequency background electrical activity (van Mierlo et al., 2013). Complex Morlet wavelet time-frequency analysis was performed to ensure ictal activity, across all analyzed seizures, occurred within the chosen frequency range (Qin et al., 2004). Fig. 6 shows illustrative time-frequency energy

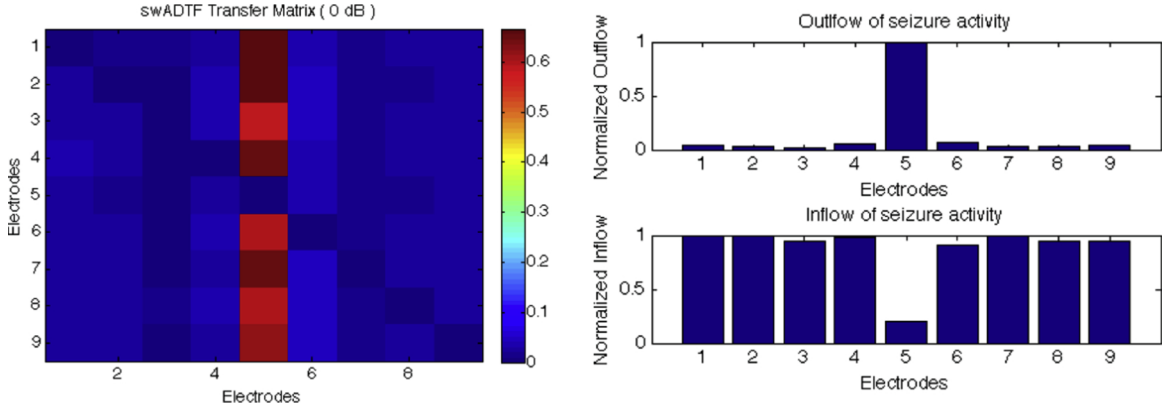

Fig. 4. Simulation results: swADTF transfer matrix (left), outflow (right, top) and inflow (right, bottom) of seizure activity.

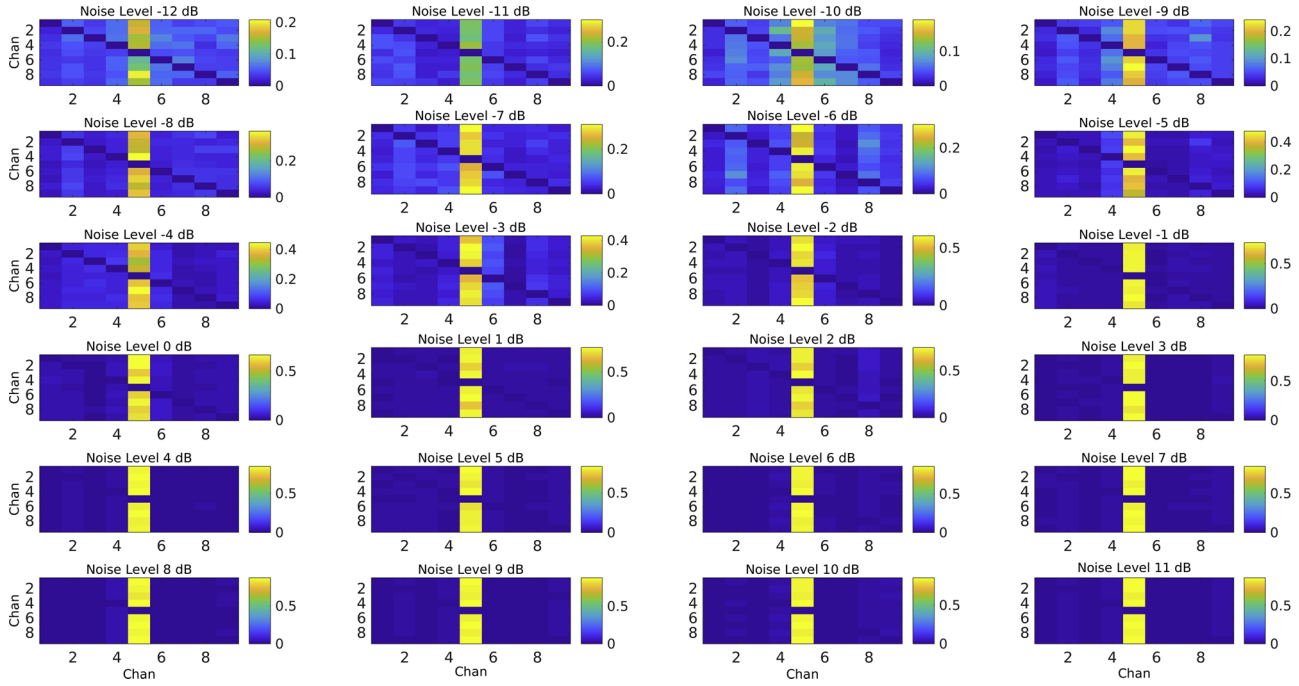

Fig. 5. Simulation results with Gaussian white noise added to iEEG ($-12\,\text{dB} \leq \text{SNR} \leq 11\,\text{dB}$): The swADTF is stable in identifying node 5 as the generator of seizure activity. Noise simulation results highlight swADTF's resistance to noise for a SNR as low as $-12\,\text{dB}$; Chan: channels.

distribution of seizure onset patterns for patients 1, 2, and 3.

The 5-sec frame prior to seizure onset was discarded from the analysis. It was only included to let the Kalman filter adapt to the iEEG recordings. Outflow and inflow of seizure activity were extracted from the time and frequency integrated swADTF transfer matrices. Model orders were subject and seizure specific; they ranged between 1 and 10 with an average of 3.

Phase shuffling-based surrogate data testing was repeated 1000 times and an average of 97.76 causal relations (channel combination) per seizure (min: 15, max: 330) passed the 0.05 significance level.

Table 2 depicts results for all patients in terms of regions selected by visual analysis, resected region, as well as swADTF-identified ictal generators and sinks. For patients with Engel I outcome, and for whom the resected region was sampled by iEEG contacts, ictal generators were within the resected volume and among electrode contacts visually identified by the expert epileptologist. Note however that for patient 1, swADTF identified three ictal generators (different generator for each seizure) from three distinct non-contiguous areas, only one of which was resected to provide seizure freedom. For the remaining two patients (#6 and #7) with poor post-operative seizure outcome, the identified ictal generators were outside of the resected region. For patient 6, while the parietal operculum was resected, two nearby contacts in the anterior insula and inferior frontal gyrus with quasi-similar outflow scores were not. For patient 7, the identified generator in the superior temporal gyrus was right below the resected area (anterior insula).

3.3. Individual results

In this section, illustrative cases of patients are discussed. Inflow and outflow of seizure activity were plotted on individual brain surfaces as reconstructed from a T1 magnetic resonance imaging (MRI) volumetric scan using Freesurfer. Individual cortex surfaces were registered to a Desikan-Killiany anatomical atlas using Brainstorm, an open source Matlab toolbox (Tadel et al., 2011). To facilitate interpretation, inflow of seizure activity was converted from channels to brain regions. Electrodes on the vertices of a given region as well as the connectivity of pairs of electrodes between two regions were averaged.

3.3.1. Illustrative case 1

Patient 1 is a 38-year-old female who suffered from non-lesional focal epilepsy since the age of 5 years. After failing six antiepileptic drugs, she was referred for epilepsy surgery. Clinically, seizures were characterized by sudden non-mirthful laughter and complex motor

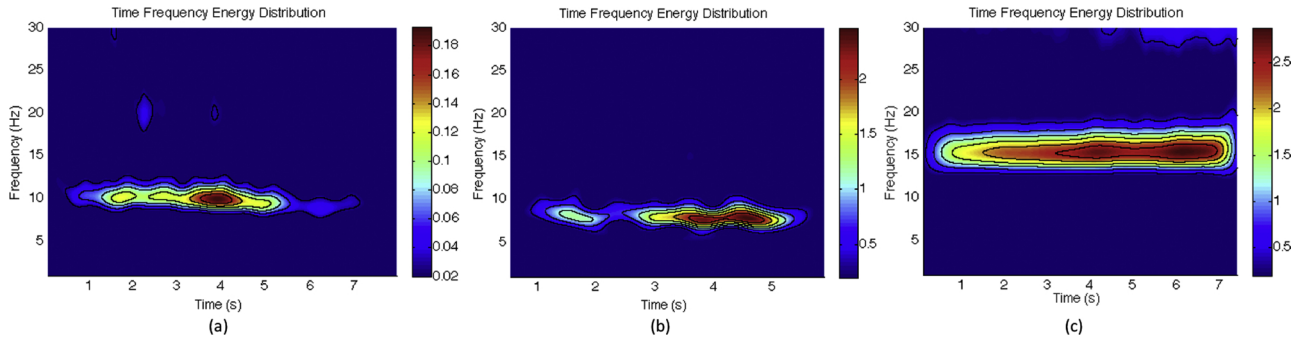

Fig. 6. Time-Frequency energy distribution for 3 different seizures of (a) Patient 1, (b) Patient 2, and (c) Patient 3 at randomly chosen electrodes. Seizure onset, as labelled by an expert epileptologist, occurred at t = 0 s.

Table 2
Group results in terms of resected regions, sources, and sinks of seizure activity.

Patient ID	SOZ	Resection: Ins/op	Seizure Semiology	Outcome (Engel)	Ictal generators	Ictal sinks
1	Ant Ins + F op	Ant and middle/FT	No aura/laughing/complex motor behavior	IA	Ant Ins + Medial OF + ant STG	Lateral OF + Fusiform + Post central gyrus
2	Post Ins	Post/T	R arm painful somatosensory symptoms/Dystonic posturing	IB	Pos Ins	Cingulate +para-central +MFG/SFG
3	Sup Ins + F op	Ant/F	No aura/laughing or swearing, complex motor behavior	IA	Medial OF	Lat OF + SFG + SPL
4	Post Ins, P op/T op	Post/PT	Diurnal: audiogenic reflex L hemiface somatosensory symptoms; Nocturnal: no aura/ complex motor behavior	IA	Pos Ins	IFG + Post-central gyrus
5	Sup Ins, F op	Ant/F	Anxiety, palpitations/R dystonic posturing and head deviation	IA	F op	Pre-central + F op
6	Post Ins, T op/P op	Post and Inf/ TP	L hemiface somatosensory, olfactory and auditory auras ± l facial clonic jerks and bilateral convulsive	IIIA	Ant Ins/P op/IFG	Ins + lat OF
7	Ant Ins, F op	Ant/-	No aura, behavioral arrest, ± bilateral convulsive	IIIA	STG	Fusiform + T Pole + Medial OF

SOZ: seizure onset zone; Ant Ins: anterior insula; F op: frontal operculum; Post Ins: posterior insula; Sup Ins: superior insula; P op: parietal opercula; T op: temporal operculum; L: left; R: right; Ins: insular; op: operculum; Ant: anterior; F: frontal: T: temporal; Rad: radical.

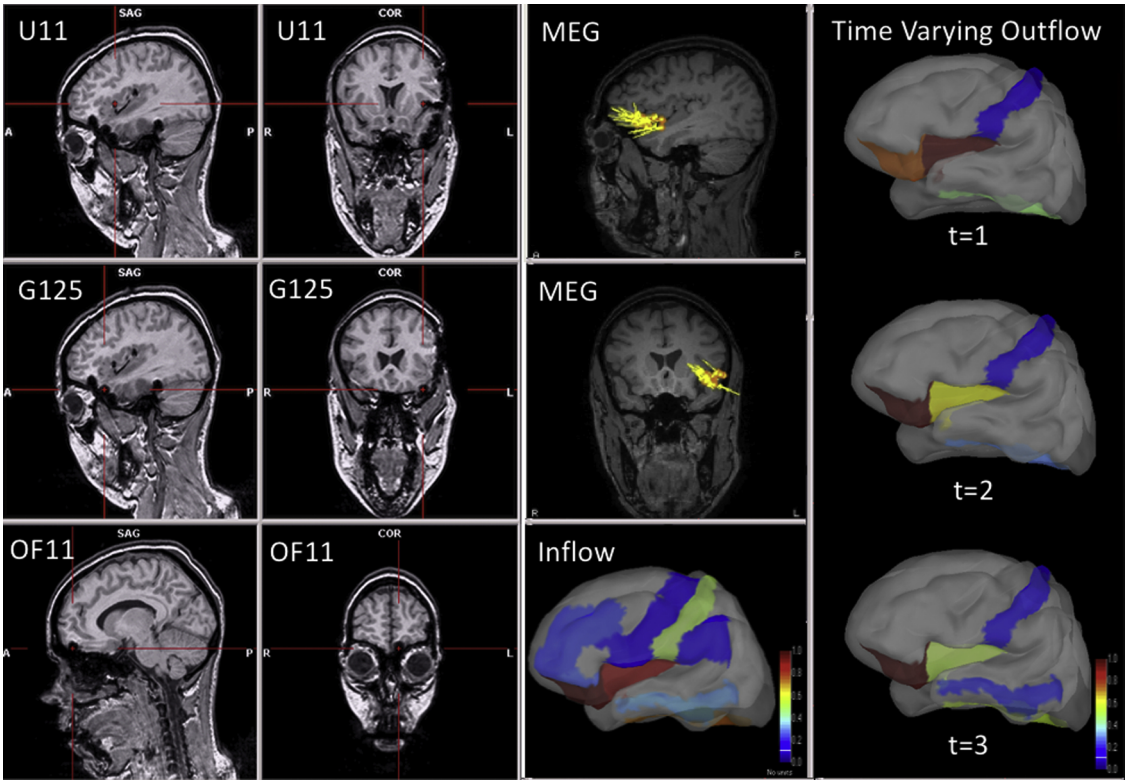

Fig. 7. Individual swADTF connectivity results for patient 1; U: insular depth electrodes, G:Grid electrodes OF: orbito-frontal strip electrode; MEG: Magnetoencephalography.

movements, suggestive of prefrontal lobe involvement. However, non-invasive investigations suggested a seizure focus in the left anterior insula (see magnetoencephalography (MEG) results in Fig. 7). An intracranial EEG subsequently confirmed a seizure onset zone in the left anterior insula extending to the frontal operculum. She underwent surgical resection of the left anterior and middle insula and part of the adjacent frontal and temporal opercula with good post-operative seizure outcome (Engel IA outcome). As mentioned in Table 2, swADTF identified three contacts (one for each individually analyzed seizure). While electrode contact U11 located in the anterior insula was within the seizure onset zone, the other two (contact OF11 in the orbitofrontal cortex and G125 in the superior temporal gyrus) were not. This may suggest that swADTF as integrated across the first seven seconds of the seizure may not always be able to distinguish a primary ictal generator from secondary ictal generators (a node with high inflow but also high outflow).

In an attempt to distinguish primary from secondary generators of seizure activity, time-varying outflow of seizure activity was plotted at

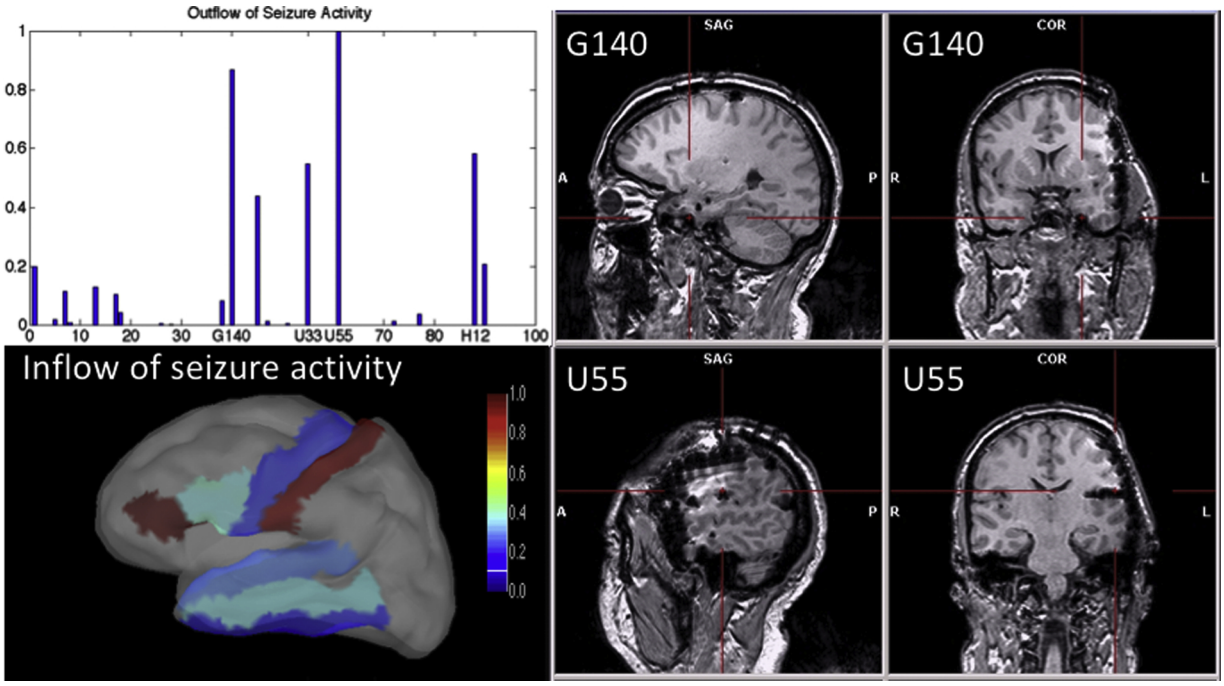

Fig. 8. Individual swADTF connectivity results for patient 4.

the early seizure onset. As shown in Fig. 7, the insula exhibited the highest outflow of seizure activity at time $t = 1$ (following electrical seizure onset); afterwards the lateral orbitofrontal gyrus becomes the highest source of seizure activity.

3.3.2. Illustrative case 2

Patient 4 is a 46-year-old male with non-lesional drug-resistant epilepsy since age 16 years. He presented diurnal seizures manifesting as paroxysmal pain over the right face often triggered by loud noises, suggestive of a focus involving the posterior insula at the junction of the secondary somatosensory cortex (pain) and the auditory cortex both in the parietal operculum, and possibly also the inferior primary sensory cortex (face sensory). He also presented sleep-related episodes with complex motor behaviours suggesting prefrontal propagation. Invasive EEG recordings confirmed the location of the seizure onset zone in the left posterior insula extending to the adjacent parietal and temporal opercula; a subsequent left operculo-insular resection led to seizure-freedom (Engel IA outcome). The electrode contact identified as the maximal source of outflow based on swADTF was indeed located within the resected volume which led to seizure-freedom (Fig. 8). Averaging inflow activity across three seizures, the highest inflow of seizure activity included the inferior frontal gyrus and the post central gyrus (where the primary and secondary somatosensory functional cortices are located). Because diurnal and nocturnal seizures were different, we individually analyzed each seizure type. As shown in Fig. 9, the analyzed nocturnal seizure which was not triggered by loud noises and featured complex motor behaviour (suggestive of prefrontal involvement) exhibited high activation of the left inferior frontal gyrus while the analyzed diurnal audiogenic reflex painful somatosensory seizure exhibited propagation to the post central gyrus (primary and secondary somatosensory cortices), the temporal neocortex and the pars opercularis.

3.3.3. Illustrative case study 3

Patient 7 is a 36-year-old male with non-lesional predominantly sleep-related epilepsy since age 31 years. Seizures were characterized by sudden awakening, fixed gaze and behavioral arrest followed by limb hypertonia. MEG and ictal single-photon emission computed tomography (SPECT) (Fig. 10) suggested a left operculo-insular focus. Intracranial EEG revealed interictal broadly distributed spikes involving the anterior insula, the frontal operculum, the orbitofrontal cortex and temporal areas. Seizures started with a broadly distributed spike and wave discharge followed by relatively diffuse low-voltage fast activity involving several contacts. Based on visual analysis, maximum evolution was felt to be in the anterior insula, inferior frontal gyrus, superior temporal gyrus, and orbitofrontal gyrus. The anterior insula and frontal operculum were resected (sparing Broca's language area) with a worthwhile seizure reduction but not seizure freedom (Engel III outcome). Interestingly, swADTF analysis identified the maximum outflow of seizure activity in the superior temporal gyrus which was not part of the resection volume. The region exhibiting highest inflow of seizure activity was the fusiform gyrus, the temporal pole and the medial orbitofrontal gyrus.

4. Discussion

In this work, we have investigated the ability of the swADTF in identifying seizure foci in patients with apparent operculo-insular seizures. More specifically, we applied the swADTF to iEEG recordings of seven patients with insular epilepsy who underwent an operculo-insular resection guided by iEEG findings, five of whom with subsequent good outcome and 2 with poorer outcome. To our knowledge, this is the first study to use multivariate autoregressive modeling based effective connectivity for the analysis of operculo-insular seizures.

For four of the five patients with good outcome, swADTF-identified the electrode contact exhibiting highest outflow within the resected volume. For one of these four patients however, more than one electrode contact was identified as a possible generator. For this patient (#1), three different non-contiguous electrode contacts were identified, indicating that swADTF as integrated across the first seven seconds of the seizure may not always be able to distinguish a primary ictal generator from secondary ictal generators and that visual inspection of the time-varying outflow of seizure activity may be necessary. We are currently evaluating the feasibility of using clustering/classification approaches to quantitatively identify primary from secondary generators of seizure activity. Regarding the single patient with good outcome for whom swADTF identified a generator in the medial orbitofrontal gyrus rather than in the insula, it should be noted that the

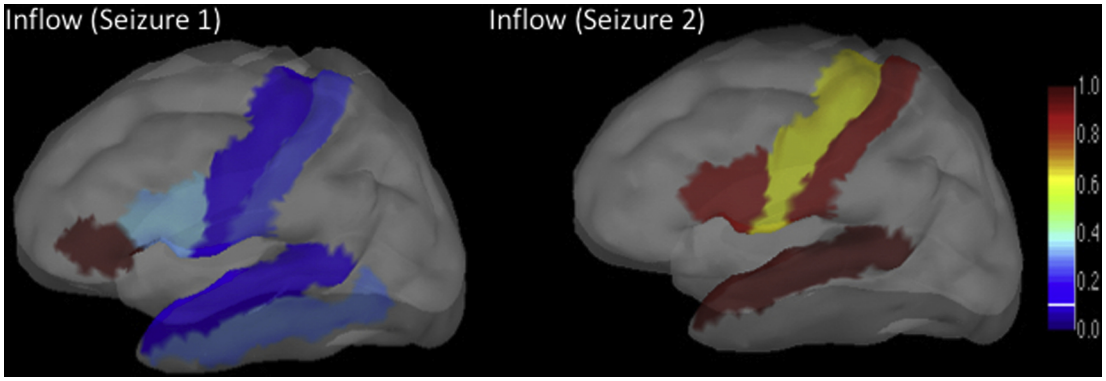

Fig. 9. Seizure specific swADTF analysis for patient 4. Seizure 1 is a sleep-related seizure characterized by complex motor behavior semiology while seizure 2 is a diurnal seizure starting with somatosensory symptoms.

depth electrode initially destined to reach the anterior insula was found to be located on the post-implantation MRI in the posterior insula close to the second depth electrode positioned in the posterior insula (as intended). This is a reminder that swADTF cannot obviously identify the ictal generator if the epileptic zone is not sampled. However, the identified generator was located within the iEEG-sampled region close to the anterior insula (resected region-not sampled by iEEG contacts for this patient). Structural connectivity results from our group have suggested that the orbitofrontal gyrus and anterior insula are highly connected brain regions (Ghaziri et al., 2017). For the final two patients with a poor post-operative seizure outcome, the swADTF-identified contact of maximum outflow was outside the surgical volume, suggesting resection of the wrong area or only part of it (albeit this cannot be verified as both patients declined a second iEEG study). Our observations are in line with previous investigations applying the swADTF to patients with other types of focal epilepsy (van Mierlo et al., 2013). In a series of 8 temporal lobe epilepsy patients operated successfully (Engel I outcome), Van Mierlo et al. (2013) showed that the electrode contact with the highest outflow, so called “driver”, was within the region clinically identified as the epileptogenic zone and resected volume (van Mierlo et al., 2013). In another series of eleven pediatric patients with frontal or parietal lobe epilepsies, Wilke et al. (2010)

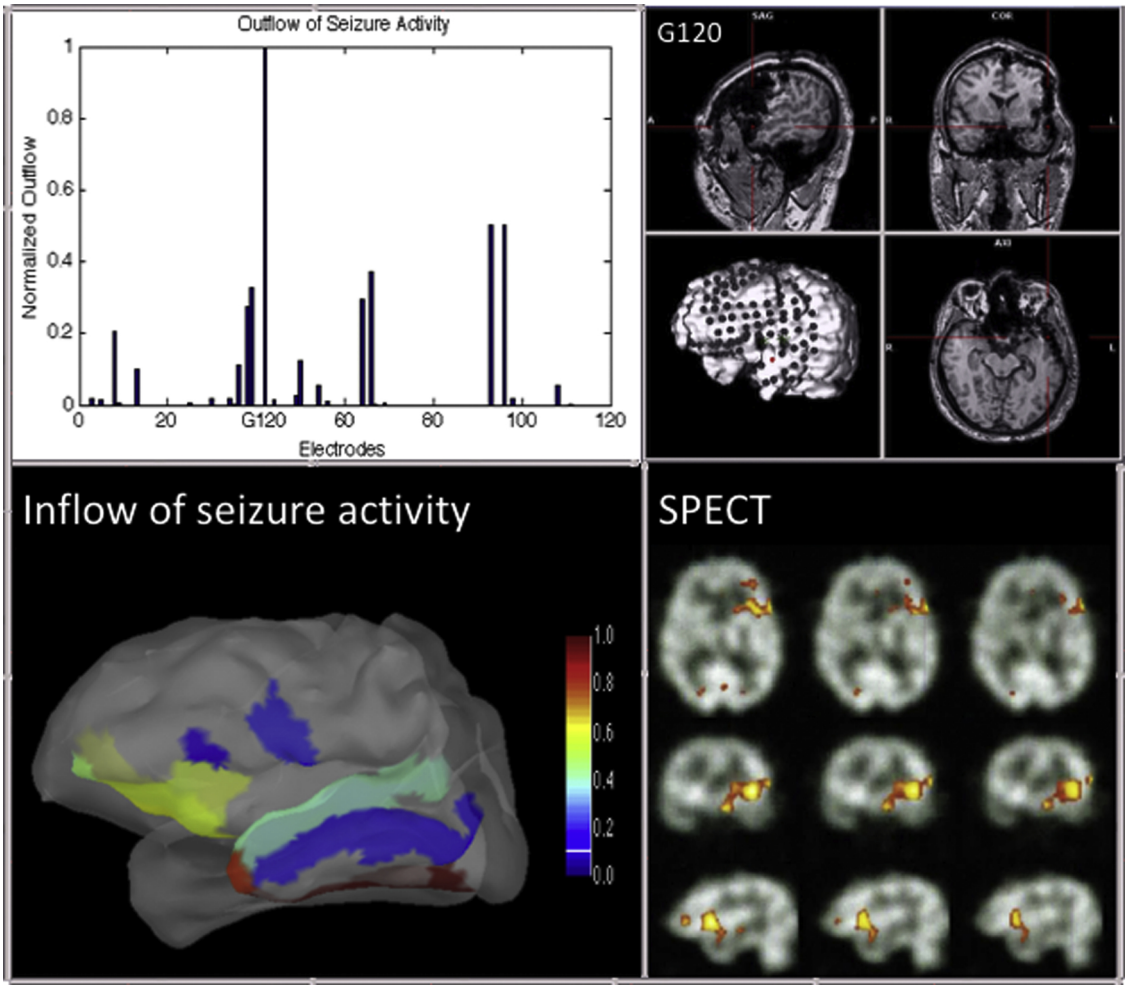

Fig. 10. Individual swADTF connectivity results for patient 7; SPECT: single-photon emission computed tomography.

applied the DTF to selected quasi-stationary iEEG epochs and integrated the transfer matrix across the frequency range of interest (as identified by means of Morlet wavelet-based time frequency analysis) (Wilke et al., 2010). They showed that electrode contacts with normalized outflow values higher than 0.8 (DTF-identified generators) highly correlated with seizure onset zones identified by expert epileptologists.

Although very preliminary, initial observations also suggest that regions identified as generators (defined as the contact of maximal outflow) or sinks (defined as areas of with inflow values higher than 80% of the maximum calculated inflow across areas) of seizure activity, appeared to correlate with seizure semiology. For the three patients who exhibited somatosensory auras (#2, 4, and 6), all had ictal generators in the posterior insula or parietal operculum which are known to produce such symptoms when electrically stimulated. We also note that two out of the three patients with complex motor behaviours (#1 and 2) had sinks of seizure activity in the orbitofrontal cortex (an area which is typically expected to be involved during such manifestations, in addition to the medial prefrontal region); the third (#3), who did not have electrodes sampling the orbitofrontal cortex nor the medial prefrontal region, had an identified-sink in the nearby inferior frontal gyrus.

Our study has some merit and limitations. First, the recordings we used to perform multivariate effective connectivity were obtained from a high number of intracranial electrode contacts (mean of 95) sampling a number of brain areas. Previous investigations used a limited number of electrodes (Martinez-Vargas et al., 2017), shorter analysis segments (Wilke et al., 2010), or visually identified regions of interest (Hagiwara et al., 2017; van Mierlo et al., 2013). Still, we acknowledge that some of regions of interest were probably not recorded. Computational requirements of adaptive multivariate modeling with surrogate based statistical validation can constitute a major constraint. In this work, we took advantage of high computational capabilities (160 cores, 1TB RAM, IBM X3850 × 5, 8* Intel E7-8870 CPU) to include all implanted electrodes in swADTF analysis. In addition, simulations were optimized and parallelized over available cores using Matlab© parallel computing toolbox. Despite computational requirements, the swADTF is preferred as compared to other quantitative measures based on Granger causality.

The major advantage of using the swADTF in this work is that it allows to overcome the non-stationary nature of iEEG recordings, previously considered as an issue when using traditional autoregressive modeling strategies. Wilke et al. (2010) selected a 3–7 sec window following seizure onset and employed the directed transfer function to determine the origin of neocortical extra-temporal seizures. In contrast, Wilke et al. (2008) integrated the adaptive directed transfer function over the duration of spikes (˜ 1 s). More recently, Mierlo et al. (2013) integrated the directed transfer function over the 20 s following seizure's onset. Choosing relatively short iEEG segments following seizure's onset allows focusing the analysis on early seizure initiation patterns rather than propagation and spread. Although using the swADTF for the identification of generators and sinks of seizure activity does not necessarily require selecting segments of relatively long duration, this characteristic allows employing it in other type of studies which involve the analysis of non-stationary segments of longer duration (e.g. identification of interictal networks, etc.) albeit computational requirements should be considered. For example, Vlachos et al. (2017) showed that it is possible to identify the epileptogenic zone from other regions by analyzing interictal iEEG recordings (Vlachos et al., 2017). On the other side, Krishnan et al. (2015) showed that epileptogenic focus localization is possible through connectivity analysis of interictal magnetoencephalographic data (Krishnan et al., 2015).

A non-parametric statistical test was used throughout all analyses to validate the significance of causal relations among iEEG channels. Surrogated data testing was previously proposed and used in several effective connectivity analysis-based studies (Wilke et al., 2008, 2010). The main advantage of using such an approach is that the shuffling the phases of the Fourier coefficients does not affect the spectral structure of the time series. This is of critical importance since the swADTF is a frequency-based measure.

The relatively small number of patients is another limitation. Although an increasing number of cases are being identified, operculo-insular epilepsy cases remain small in comparison with temporal or frontal lobe epilepsy. In addition, we chose to restrict ourselves to a relatively homogeneous group of patients with operculo-insular epilepsy to better understand this focal epileptic condition at times considered as a great mimicker due to the variety of associated ictal manifestations. Obviously, larger studies are necessary to reproduce our preliminary findings, both for operculo-insular epilepsy or any type of focal epilepsy.

In this work, a noise simulation analysis was performed in order to show the ability of swADTF in detecting sources and sinks of seizure activity in time-varying information flow in the presence of relatively high noise levels. Given that a white Gaussian noise has been previously proven to mostly interfere with iEEG recordings, it was added (at different SNRs) to ictal signals. Results showed that the swADTF was insensitive to such type of noise and accurately identified the epileptic networks in all cases. Considering that a Gaussian noise is a stationary process, care must be taken when considering other types of noise especially those adding time-varying fluctuations to the iEEG signal. Assessing the effect of non-stationary noises on the performance of the swADTF is a tempting avenue but goes beyond the scope of this manuscript.

The use of intracranial EEG recordings reduces the effect of volume conduction; however the effect of mutual sources can easily introduce spurious connectivity within iEEG channels. Unfortunately, this issues is encountered in all connectivity analyses; it was mitigated in this work by: (1) using a multivariate rather than a bivariate analysis/ modeling strategy and (2) using a non-parametric statistical test (surrogate data testing) with a significance level of 5% and a phase shuffling of 1000 times.

In line with previous investigations, a single electrodes was identified as the generator/source while a threshold of 80% of the maximal inflow was used to find sinks of seizure activity. Future work will address the effect of using different threshold on the results as well as the feasibility of non-supervised clustering based approaches.

Recent studies have demonstrated that high frequency oscillations (HFOs) may be correlated with the seizure onset zone. Due to limitations imposed by under sampling iEEG time series to cope with computational requirements, we were unable to study interactions within HFOs. Future perspectives include additional processing and swATDF computational optimization to study seizure onset patterns within HFOs.

5. Conclusions

In this work we examined the ability of the swADTF in localizing the seizure onset zone in patients with apparent operculo-insular epilepsy. Preliminary results showed that, despite the rapid spread of seizure activity, swADTF is a promising tool to complement visual assessment of seizure origin and propagation. Caveats include adequate sampling by electrode contacts of suspected areas of epileptogenicity, separately analyzing different seizure types if more than one seizure focus is suspected, and using a time-varying outflow representation when swADTF is unable to distinguish a primary ictal generator from secondary ictal generators. Larger prospective studies are obviously necessary before considering translation into clinical practice.

Acknowledgements

Authors acknowledge financial support from the Natural Sciences and Engineering Research Council of Canada, Epilepsy Canada and the Institute for Data Valorization (IVADO). DKN holds the Canada Research Chair in Epilepsy and Functional anatomy of the Human Brain.

References

Assi, E.B., Sawan, M., Nguyen, D.K., Rihana, S., 2016. A 2D clustering approach investigating inter-hemispheric seizure flow by means of a directed transfer function. 6-7 Oct. 2016. Paper Presented at the 2016 3rd Middle East Conference on Biomedical Engineering (MECBME).

Engel, J., 1993. Update on surgical treatment of the epilepsies. Neurology 43 (8), 1612. https://doi.org/10.1212/WNL.43.8.1612.

Ghaziri, J., Tucholka, A., Girard, G., Houde, J.-C., Boucher, O., Gilbert, G., et al., 2017. The corticocortical structural connectivity of the human insula. Cereb. Cortex 27 (2), 1216–1228. https://doi.org/10.1093/cercor/bhv308.

Hagiwara, K., Jung, J., Bouet, R., Abdallah, C., Guénot, M., Garcia-Larrea, L., et al., 2017. How can we explain the frontal presentation of insular lobe epilepsy? The impact of non-linear analysis of insular seizures. Clin. Neurophysiol. 128 (5), 780–791. https://doi.org/10.1016/j.clinph.2017.01.022.

Harroud, A., Bouthillier, A., Weil, A.G., Nguyen, D.K., 2012. Temporal lobe epilepsy surgery failures: a review. Epilepsy Res. Treat. 2012 (2090–1356 (Electronic)).

He, B., Dai, Y., Astolfi, L., Babiloni, F., Yuan, H., Yang, L., 2011. eConnectome: a MATLAB toolbox for mapping and imaging of brain functional connectivity. J. Neurosci. Methods 195 (2), 261–269. https://doi.org/10.1016/j.jneumeth.2010.11.015.

Jia, H., Hu, X., Deshpande, G., 2014. Behavioral relevance of the dynamics of the functional brain connectome. Brain Connect. 4 (9), 741–759. https://doi.org/10.1089/brain.2014.0300.

Kaminski, M., Ding, M., Truccolo, W.A., Bressler, S.L., 2001. Evaluating causal relations in neural systems: granger causality, directed transfer function and statistical assessment of significance. Biol. Cybern. 85 (2).

Klamer, S., Rona, S., Elshahabi, A., Lerche, H., Braun, C., Honegger, J., et al., 2015. Multimodal effective connectivity analysis reveals seizure focus and propagation in musicogenic epilepsy. NeuroImage 113, 70–77. https://doi.org/10.1016/j.neuroimage.2015.03.027.

Krishnan, B., Vlachos, I., Wang, Z.I., Mosher, J., Najm, I., Burgess, R., et al., 2015. Epileptic focus localization based on resting state interictal MEG recordings is feasible irrespective of the presence or absence of spikes. Clin. Neurophysiol. 124 (6).

Levy, A., Tp, Yen Tran, Boucher, O., Bouthillier, A., Nguyen, D.K., 2017. Operculo-insular epilepsy: scalp and intracranial electroencephalographic findings. J. Clin. Neurophysiol. 34 (5).

Martinez-Vargas, J.D., Strobbe, G., Vonck, K., van Mierlo, P., Castellanos-Dominguez, G., 2017. Improved localization of seizure onset zones using spatiotemporal constraints and time-varying source connectivity. Front. Neurosci. 11, 156. https://doi.org/10.3389/fnins.2017.00156.

Obaid, S., Zerouali, Y., Nguyen, D.K., 2017. Insular epilepsy: semiology and noninvasive investigations. J. Clin. Neurophysiol. 34 (4), 1537–1603 (Electronic).

Paris, A., Atia, G.K., Vosoughi, A., Berman, S.A., 2017. A new statistical model of electroencephalogram noise spectra for real-time brain– computer interfaces. IEEE Trans. Biomed. Eng. 64 (8), 1688–1700. https://doi.org/10.1109/TBME.2016.2606595.

Qin, L., Ding, L., He, B., 2004. Motor imagery classification by means of source analysis for brain-computer interface applications. J. Neural Eng. 1 (3).

Tadel, F., Baillet, S., Mosher, J.C., Pantazis, D., Leahy, R.M., 2011. Brainstorm: a user-friendly application for MEG/EEG analysis. Comput. Intell. Neurosci. 13. https://doi.org/10.1155/2011/879716. 2011.

Uddin, L.Q.S., Hebert-B, N.J., Ghaziri, J., Boucher, O., 2017. Structure and function of the human insula. J. Clin. Neurophysiol. 34 (4).

van Mierlo, P., Carrette, E., Hallez, H., Raedt, R., Meurs, A., Vandenberghe, S., et al., 2013. Ictal-onset localization through connectivity analysis of intracranial EEG signals in patients with refractory epilepsy. Epilepsia 54 (8), 1409–1418. https://doi.org/10.1111/epi.12206.

Vlachos, I., Krishnan, B., Treiman, D.M., Tsakalis, K., Kugiumtzis, D., Iasemidis, L.D., 2017. The concept of effective inflow: application to interictal localization of the epileptogenic focus from iEEG. IEEE Trans. Biomed. Eng. 64 (9), 2241–2252. https://doi.org/10.1109/TBME.2016.2633200.

Wilke, C., Ding, L., He, B., 2008. Estimation of time-varying connectivity patterns through the use of an adaptive directed transfer function. IEEE Trans. Biomed. Eng. 55 (11).

Wilke, C., van Drongelen, W., Kohrman, M., He, B., 2010. Neocortical seizure foci localization by means of a directed transfer function method. Epilepsia 51 (4).